

P12.6 AN EXPLORATORY STUDY OF MODELING ENROUTE PILOT CONVECTIVE STORM FLIGHT DEVIATION BEHAVIOR[†]

Rich DeLaura*
James Evans
Massachusetts Institute of Technology, Lincoln Laboratory
244 Wood Street
Lexington, MA 02420

1. ABSTRACT

The optimization of traffic flows in highly congested airspace with rapidly varying convective weather is an extremely complex problem. Aviation weather systems such as the Corridor Integrated Weather System (CIWS) provide weather products and forecasts that aid en route traffic managers in making tactical routing decisions in convective weather, but traffic managers need automated decision support systems that integrate flight information, trajectory models and convective weather products to assist in developing and executing convective weather mitigation plans.

A key element of an integrated ATM/wx decision support system is the ability to predict automatically when pilots in en route airspace will choose to deviate around convective weather and how far they will deviate from their planned path. The FAA Aeronautical Information Manual suggests that pilots avoid thunderstorms characterized by “intense radar echo” in en route airspace by at least 20 nautical miles (40 km). However, a recent study (Rhoda, et. al., 2002) of pilot behavior in both terminal and en route airspace near Memphis, TN suggested that pilots fly over high reflectivity cells in en route airspace and penetrate lower cells whose reflectivity is less than VIP level 3. Recent operational experience with CIWS supports the Rhoda findings (Robinson, et. al., 2004).

This study presents initial results of research to develop a quantitative model that would predict when a pilot will deviate around

convective weather in en route airspace. It also presents statistics that characterize hazard *avoidance distances* and weather penetrations. The results are based on the analysis of more than 800 flight trajectories through two Air Traffic Control (ATC) en route *super-sectors* (geographical regions that include several adjacent ATC en route sectors) on five days in the summer of 2003. One super-sector from the Indianapolis Air Route Traffic Control Center (ZID ARTCC) encompassed southern Indiana, southwestern Ohio and northern Kentucky (ZID); the other, located in the Cleveland ARTCC (ZOB), included northern Ohio, along the southern shore of Lake Erie (ZOB). The weather encountered along the flight trajectories was characterized by the CIWS high-resolution precipitation (VIL) and radar echo tops mosaic (Klinge-Wilson and Evans, 2005) and NLDN lightning products. Flight trajectories were taken from the Enhanced Traffic Management System (ETMS).

2. INTRODUCTION

Aviation weather systems such as the Corridor Integrated Weather System (CIWS) provide weather products and forecasts that aid enroute controllers in making tactical routing decisions in convective weather. However, enroute controllers need tools to aid them in the significant effort required to use the weather information to develop and execute a comprehensive plan to route traffic through the weather. Critical tasks – such as determining the impact of weather on existing traffic, devising a tactical response to mitigate the impacts of weather, predicting the effects of a particular routing strategy, predicting arrival times for flights traversing regions of convective weather – significantly increase controller workload and are often executed in a suboptimal manner due to the complexity of the tasks. Furthermore, different decision makers may reach very different conclusions about weather impact, etc. because the subjective judgment of the decision maker is the primary ‘tool’ used to perform these tasks. A comprehensive decision support system that provides automated tools that integrate flight information, trajectory models and weather

[†]This work was sponsored by the National Aeronautics and Space Administration (NASA) under Air Force Contract FA8721-05-C-0002. Opinions, interpretations, conclusions, and recommendations are those of the authors and are not necessarily endorsed by the United States Government.

* *Corresponding author address:* Rich DeLaura, MIT Lincoln Laboratory, 244 Wood Street, Lexington, MA 02420-9185; e-mail: richd@ll.mit.edu

forecasts should help air traffic personnel make better and more pro-active decisions while reducing workload during convective events.

An important component in an integrated decision support system is the ability to predict when pilots in enroute airspace will choose to deviate around convective weather and how far they will deviate from their planned path. The FAA Aeronautical Information Manual suggests that pilots avoid thunderstorms characterized by “intense radar echo” in enroute airspace by at least 20 miles (40 km). However, a recent study (Rhoda, et. al., 2002) suggests that pilots fly over high reflectivity cells in enroute airspace and penetrate lower reflectivity cells. Recent operational experience with CIWS in enroute airspace (Robinson, et. al., 2004) supports the observations of (Rhoda, et. al., 2002).

This study presents initial results of a study to develop a quantitative statistical model that predicts pilot deviation behavior in enroute airspace owing to convective weather. Data used in this study came from five different days in the summer of 2003 with significant convective weather in two different ‘super-sectors’ (regions defined by a small group of adjacent Air Traffic Control enroute sectors). An automated process extracted enroute flight trajectories from the Enhanced Traffic Management System (ETMS) and calculated the planned trajectory corresponding to each actual flight trajectory extracted. A second automated analysis, the deviation detection algorithm, identified planned trajectories that encountered significant weather and determined if the aircraft significantly deviated from the planned trajectory. The results of the automated deviation detection algorithm were reviewed and edited by a human analyst. The edited deviation detection results and several statistical measures of the weather encountered along the planned trajectories (automatically extracted from CIWS weather data) provided the inputs to the deviation prediction model.

In addition to the deviation prediction model, this study presents an analysis of deviating flight trajectories and statistics that provide insight into deviation strategies. The avoidance distance (the distance from the boundary of the weather feature around which the pilot is deviating) was calculated for each deviating trajectory. The importance of deviation distance as a key factor in assessing ATC impact is illustrated graphically in the studies of “convectively constrained areas (CCAs)” that have been

carried out in the context of validation of the Collaborative Convective Forecast Product (CCFP) (Mahoney, et. al, 2004). The figures in (Mahoney, et. al., 2004) show that assuming aircraft will seek to stay at least 10 nmi away from any individual storm cell results in a very significant reduction in the usable airspace.

Finally, the study provides additional statistics about the weather that pilots actually encountered in enroute airspace. The paper concludes with recommendations for follow-on studies.

3. ANALYSIS METHODS

There were five steps in the deviation data analysis and model development:

1. Filter ETMS flight data to extract enroute flights and their actual and planned trajectories
2. Define operationally significant flight path deviation based on analysis of trajectories in clear weather
3. Calculate statistics that characterize weather encountered on planned and actual trajectories
4. Detect trajectory encounters with significant weather and weather-related deviations
5. Develop statistical model to predict deviations as a function of the input weather statistics

A flight was considered to be enroute through a super-sector (step 1) if its planned trajectory spent at least 15 minutes inside the super-sector boundaries and maintained an altitude greater than 25 kft for the complete trajectory. The planned trajectory was determined by applying the actual trajectory ground speed to the path defined by connecting the flight plan fixes from ETMS.

We defined deviation (step 2) as a flight trajectory whose mean *deviation distance* is greater than some deviation distance threshold. The deviation distance is the distance from each point on the planned trajectory to the nearest point on the actual trajectory. The *deviation threshold*, which represents the limits of normal operational variation in flight trajectories along the planned routes, was determined for each super-sector by an analysis of planned and actual trajectories on a single clear-air day: after trajectories with obvious short-cuts and re-routes were removed, the deviation threshold was defined as the 90th percentile of the mean deviation distance for the remaining trajectories.

Three CIWS products were used to characterize the weather (step 3):

1. Vertically Integrated Liquid (VIL): CIWS uses VIL as a measure of precipitation (see Robinson, et. al., 2002 for a discussion of why VIL is preferred). VIL is mapped to an equivalent 6-level Video Integrator and Processor (VIP) scale of precipitation intensity (Troxel and Engholm, 1990). In this study, a higher resolution CIWS VIL product (the precursor to the 6 level display product) was used, so fractional VIP levels could be resolved.
2. High resolution radar echo tops: measure of storm cell height (Smalley et. al., 2003)
3. Cloud-to-ground lightning strikes: measure of convective activity

For each weather encounter, weather statistics were calculated from two different sized neighborhoods, centered on the trajectory: 16km (approximating the clear-air route width) and 60km (approximating the 20 nm convective storm avoidance guidance given to pilots in the FAA Airman's Information Manual). Figure 1 illustrates the different route width scales.

The weather statistics included mean, 90th percentile and maximum values for VIL and echo tops for both neighborhoods. For the 60km neighborhood, we calculated several additional statistics, including percentage of area covered by VIL levels \geq level 3, 4 and 5; echo tops heights \geq flight altitude, 30, 40 and 50 kft; and lightning counts in 6 minute time periods. A total of 31 statistical measures of weather characteristics were calculated.

A weather encounter (step 4) was defined as a portion of a trajectory that passed through *either* VIL level 2 or greater *or* echo tops of 25 kft or greater for at least 2 minutes. The choice of VIL, echo top height and thresholds was based on a prior analysis of deviations around convective storms in enroute airspace (Rhoda, et. al., 2002). Note that the weather encounter is not intended to be an *a priori* definition of convection or weather hazard. Rather, it is the definition of the *minimum* level of weather significant enough to be analyzed.

A planned trajectory weather encounter was flagged as a weather-related deviation if the mean deviation distance during the encounter was greater than the deviation threshold calculated in step 2. This set of automatically detected weather encounters and deviation flags were reviewed by an analyst and the deviation flags were edited when necessary.

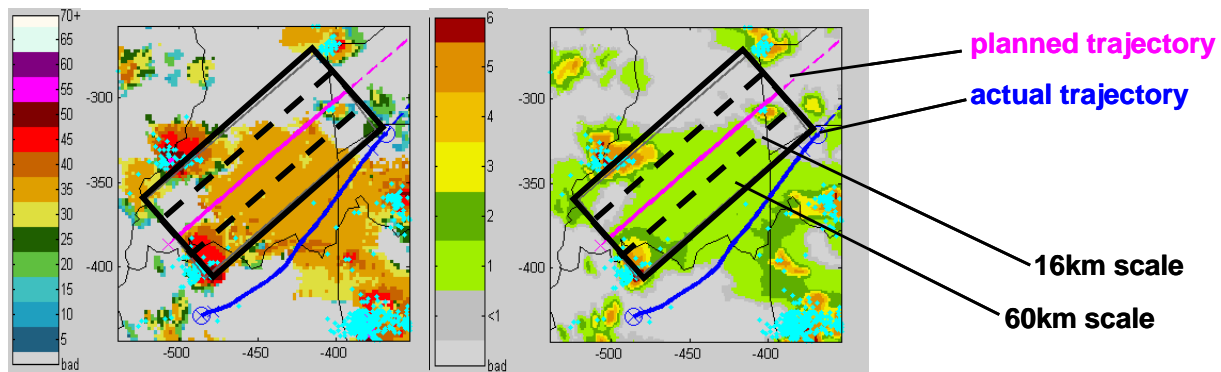


Figure 1. Illustration of different route width scales used in the extraction of weather data and calculation of weather statistics along planned and actual flight trajectories (example shows a planned trajectory neighborhood). Figure at left shows echo tops field, at right is VIL, cyan dots indicate cloud-to-ground lightning strikes.

The weather statistics and edited deviation flags from 595 weather encounters on 5 different

summer days in 2003 provided the inputs to the deviation prediction model (step 5). Twenty different

models were developed using the LNKnet pattern classification software developed at Lincoln Lab (Lippmann, et. al., 1993). In each model, a set of 5 weather statistics for each weather encounter (chosen from the complete set of 31) provided the inputs: two measures of VIL (one from the 16km neighborhood, the other from the 60km neighborhood), two measures of echo top height or *deltaZ* (flight altitude – echo top height), and lightning counts from the 60km neighborhood. In order to test the assertion that both VIL and echo tops play a part in pilot decision, we developed twelve additional models with sets of 3 inputs: lightning and *either* echo tops *or* VIL. In all models, we were careful to select sets of input variables that showed relatively low levels of cross-correlations. We compared two different pattern classifiers: k-nearest neighbors, with several different values of k, and Gaussian. The Gaussian classifier proved to be the better of the two, and all models used Gaussian classifiers. In addition to predicting output class (in this case, deviation or non-deviation), LNKnet also evaluates the explanatory power of each input variable by calculating the reduction in output classification error due to each input variable. A weather statistic that has high explanatory power in a deviation prediction model which has a small output classification error is deemed to be an important factor in pilot decision.

In order to describe deviation strategies for the verified deviations, an analyst reviewed the actual trajectories flown and the weather they encountered for 218 weather-related deviations. Each deviation was characterized by an *avoidance distance* from 24 different weather features (the minimum lateral distance between the deviating plane and the boundary of the weather feature that the pilot is avoiding). Weather features included VIL level 2, 3, 4 and 5 contours, echo top height of flight altitude, 30, 40 and 50 kft contours, and all VIL and echo top combinations. Avoidance distances were determined from a single *characteristic cross-section* chosen by the analyst to represent the weather encounter. The characteristic cross section is a line connecting the planned and actual trajectories, that spans the weather feature responsible for the deviation, in the analyst's judgment (see Figure 10 below). Statistics describing avoidance distances are presented.

4. RESULTS

4.1 Case Analysis

Flight trajectories in two 'super-sectors', ZID and ZOB, were analyzed. The ZID super-sector consisted of ATC sectors ZID66, ZID82 and ZID83; ZOB included ATC sectors ZOB28, ZOB46, ZOB48 and ZOB77. Figure 2 illustrates the super-sectors, showing the major enroute jetways and fair weather traffic in each. The majority of ZOB routes and traffic flow are carried along several parallel and closely spaced East-West oriented jetways. ZID traffic, by comparison, is evenly distributed among several jetways with different orientations. Demand, jetway orientations and spacing between jetways will all impact the way that ATC manages flow and may constrain the deviation options in convective weather.

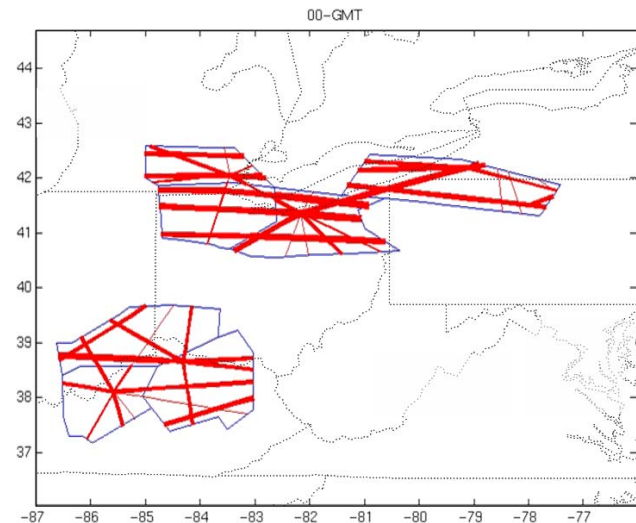


Figure 2. Jetways and clear day traffic in super-sectors ZOB and ZID. Thickness of red lines indicates traffic load.

A total of 472 enroute trajectories in ZID and 539 in ZOB during a clear 24-hour period (July 25, 2003) were analyzed to determine the deviation threshold. The deviation thresholds were 12 km for ZID and 24 km for ZOB. We found the difference in deviation thresholds between the two super-sectors somewhat surprising and can only speculate about the reasons for the difference. It may be possible that the differences are due simply to sampling errors and would disappear with the analysis of additional clear-air days. It may also be possible that the even distribution of traffic on a large number of crossing routes in the ZID super-sector presents a more complex air traffic routing problem and requires

stricter adherence to the published routes. In any event, we cannot readily explain the clear-air differences using the available data.

Table 1 presents a summary of the case dates and times, the number of flights analyzed, the number of flights whose *planned* trajectories encountered significant weather, the total number of weather encounters detected and analyzed and the median and 90th percentile of VIL and echo tops measurements from the 16km neighborhoods for all weather encounters. (Note that some trajectories may have multiple weather encounters, so that the number of weather encounters on a given day may exceed the number of trajectories with weather encounters. Note also that some weather encounters were filtered out of the analysis because they were too brief, resulting in days where the number of weather encounters is less than the number of trajectories with weather encounters.) In general, convection in ZID was stronger, with echo tops and VIL levels significantly higher than what was observed in ZOB. Storm cells in ZID were also more clearly defined, with sharp boundaries between convective cells and areas of clear weather.

Figure 3 illustrates a typical storm deviation, identified by the automatic detection algorithm. In this example, convective storm cells are characterized by high VIL, echo tops well above the flight level and lightning activity. Cell complex boundaries are readily evident, and flight trajectories clearly deviate around vigorous

convective activity. Many weather encounters and deviations in the ZID super-sector exhibited similar characteristics in all five cases.

Weather encounters in ZOB were not so easily characterized. In the five cases studied, the weather was largely stratiform precipitation with embedded weak convective cells. Flight path deviations were also less predictable, which might be expected given the wider distribution of clear air deviation distances. Figure 4 illustrates an example.

The automated deviation detection algorithm classified planned trajectory weather encounters as weather-related deviations or non-deviations, using the methods, definitions and thresholds described above in section 2. The results of the automated deviation detection algorithm were reviewed by an analyst, who inspected every weather encounter (both deviations and non-deviations) that was identified and classified by the detection algorithm. The analyst reviewed planned and actual trajectories and VIL, echo tops and lightning strike maps in the vicinity of the weather encounter to determine if the detection algorithm was correct.

The automated algorithm detected and classified 595 weather encounters in ZID and 248 in ZOB. The analyst was able to verify the deviation flag for 490 of the encounters in ZID and 176 in ZOB. The probability of detection and false alarm rate was calculated for the automated deviation detection algorithm using the verified encounters. The performance of the deviation detection algorithm is summarized in Table 2.

Table 1
Summary of Weather Encounters for Planned Trajectories

Case start: finish	Sector	Trajectories	Trajectories with weather encounters	Weather encounters	VIL (median / 90 th pct.)	Echo tops (median/ 90 th pct.)
2003/05/10 0500 :	ZID	130	95	106	5.9 / 4.9	45 / 36
2003/05/10 1900	ZOB	168	62	69	4.5 / 2.9	33 / 26
2003/06/14 1500 :	ZID	134	67	66	5.6 / 5.0	37 / 31
2003/06/15 0000	ZOB	279	24	21	4.9 / 4.6	31 / 28
2003/06/26 2000 :	ZID	142	120	128	4.9 / 4.0	30 / 38
2003/06/27 0500	ZOB	220	151	122	4.5 / 3.4	29 / 24
2003/07/09 1600 :	ZID	219	168	220	5.8 / 4.8	46 / 37
2003/07/10 1300	ZOB	531	41	36	4.5 / 2.8	33 / 26
2003/07/31 0800 :	ZID	74	52	75	5.0 / 3.9	32 / 27
2003/07/31 1800	ZOB	223	1	0	N/A	N/A
Totals (ZID/ZOB/both)		699/1421/2120	502/279/781	595/248/843		

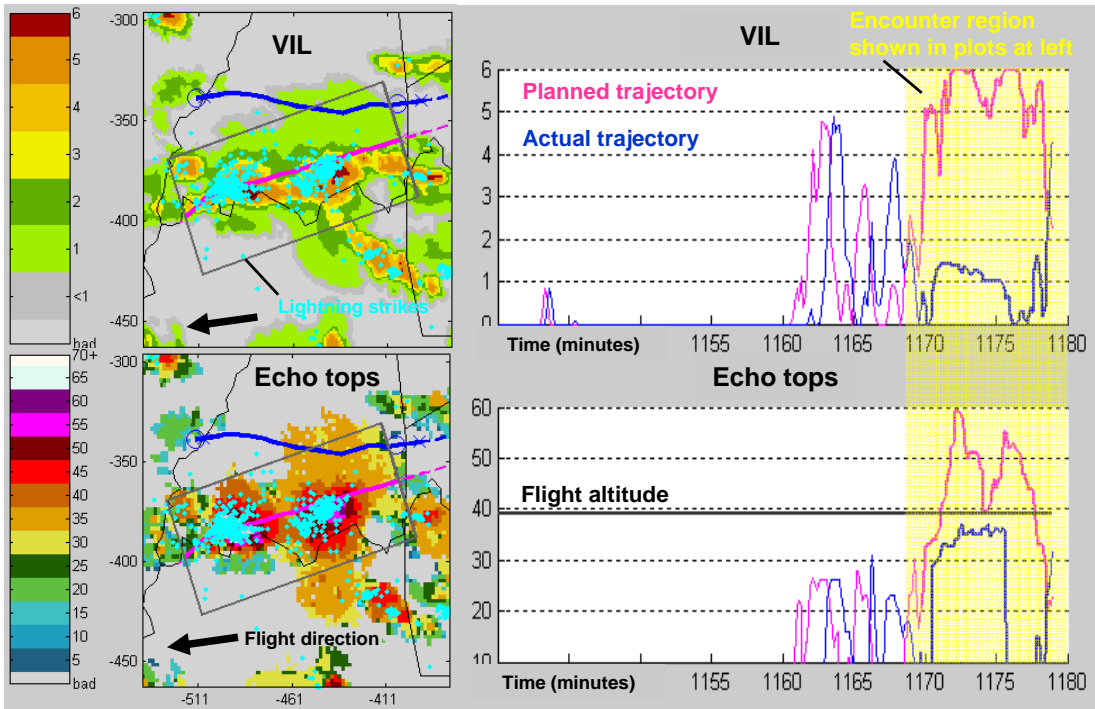


Figure 3. A typical storm cell deviation in the ZID super-sector.

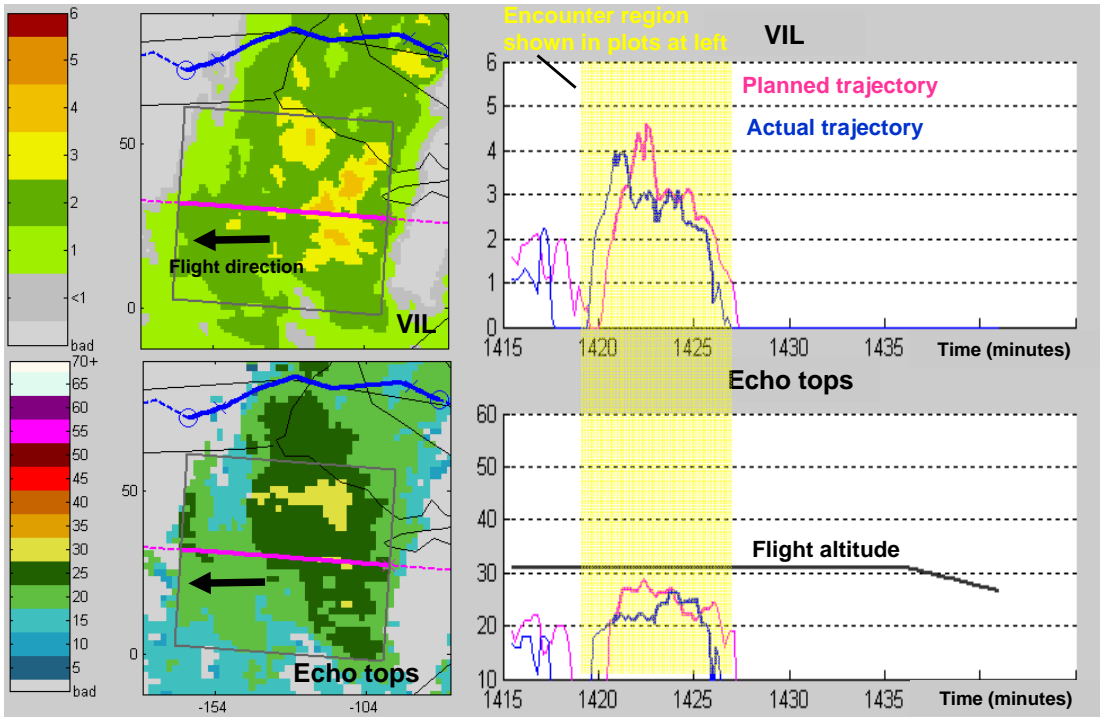


Figure 4. A typical weather-related deviation in the ZOB super-sector.

Table 2
Summary of Automated Deviation Detection Algorithm Performance

Case	Sector	Deviations POD / FAR	Non-deviations POD / FAR
2003/05/10	ZID	93.9 / 7.5	80.0 / 16.7
	ZOB	90.0 / 30.8	92.7 / 1.9
2003/06/14	ZID	86.7 / 10.3	90.9 / 11.8
	ZOB	NA / 100.0	80.0 / 0.0
2003/06/26	ZID	69.6 / 38.5	88.6 / 8.2
	ZOB	71.4 / 48.3	86.1 / 6.5
2003/07/09	ZID	94.9 / 3.7	90.2 / 13.2
	ZOB	100.0 / 40.0	81.0 / 0.0
2003/07/31	ZID	87.5 / 33.3	86.0 / 4.4
	ZOB	NA / NA	NA / NA
All cases	ZID	91.2 / 10.8	87.9 / 10.0
	ZOB	81.1 / 44.4	87.2 / 4.1

Deviation detection error rates were significantly higher in ZOB than in ZID. Several factors may have contributed to the difference in performance: clear air routes appeared to be flown much tighter in ZID¹, making the difference between deviation and non-deviation more obvious; convective cells in ZID were stronger¹ and more clearly defined in ZID than in ZOB; ATC may employ different weather avoidance strategies in the two super-sectors.

The purpose of the deviation detection algorithm is to provide the true pilot decisions to the deviation prediction model, so it was critical to ensure the accuracy of the detections. In this study, an analyst reviewed each flight to ensure that it was properly classified. The need for human review reduces the number of flights that can be analyzed, limiting the size of the data set and increasing the error in prediction models. For this reason, a reliable automated deviation detection algorithm is critical to the development of robust deviation prediction models. Further study is required to establish a clear description of the failure modes of the deviation detection algorithm and to devise improvements to address them.

4.2 Deviation Prediction Model

Inputs to the deviation prediction model consisted of 490 planned trajectory weather encounters from super-sector ZID whose

¹ This difference seems counter-intuitive given the respective route structures in ZOB and ZID.

classification (deviation or non-deviation) could be verified by the analyst. ZOB weather encounters were not considered because of the difficulty in detecting and identifying weather-related deviations, the relatively small number of encounters that deviated (32 of 176, or 18%) and the significant difference between the two super-sectors in weather characteristics and clear-air deviation thresholds.

Several general trends appeared in the results of the modeling experiments:

- 1) Overall prediction errors (both deviation and non-deviation) ranged from 19% to 26%. However, models differed significantly in the differences between deviation and non-deviation prediction errors (ranging from 2% to 28%). The better models were characterized both by low overall prediction errors and a small difference between the deviation and non-deviation prediction errors.
- 2) In 19 of the 20 modeling experiments that included both VIL and echo top measurements as inputs, the best predictor of deviation was a measure of echo top height.
- 3) In the 11 modeling experiments with the lowest overall prediction error, the best predictor was a measure of *deltaZ* (flight altitude – echo top height), based on a 90th percentile measure of echo top height within the analysis neighborhood (either 16km or 60km). The second best was a measure of VIL.
- 4) Models that used 90th percentile echo top measurements as inputs yielded results at

least as good as or better than average measurements in all cases.

- 5) Lightning appears to add little value as a predictor when both echo top height and VIL measures are available.

These general trends indicate that the **primary factor in weather-related deviations is the height of the storm relative to the flight altitude, with VIL or precip measurements reducing the difference in prediction errors for deviation and non-deviation, in some cases.** Furthermore, **spatial averaging of echo top measurements appears to reduce their predictive power.**

The results from the twelve additional models, in which lightning and only VIL or echo top measurements provided the weather inputs, were consistent with these findings. Errors for the echo top-only models were lower than those from VIL-only models.

Modeling results for all 32 models are summarized in Figure 5. The blue boxes show the overall error in predicting both deviations and non-deviations, the red show the error in predicting deviations, the green show the error in predicting non-deviations for a given model.

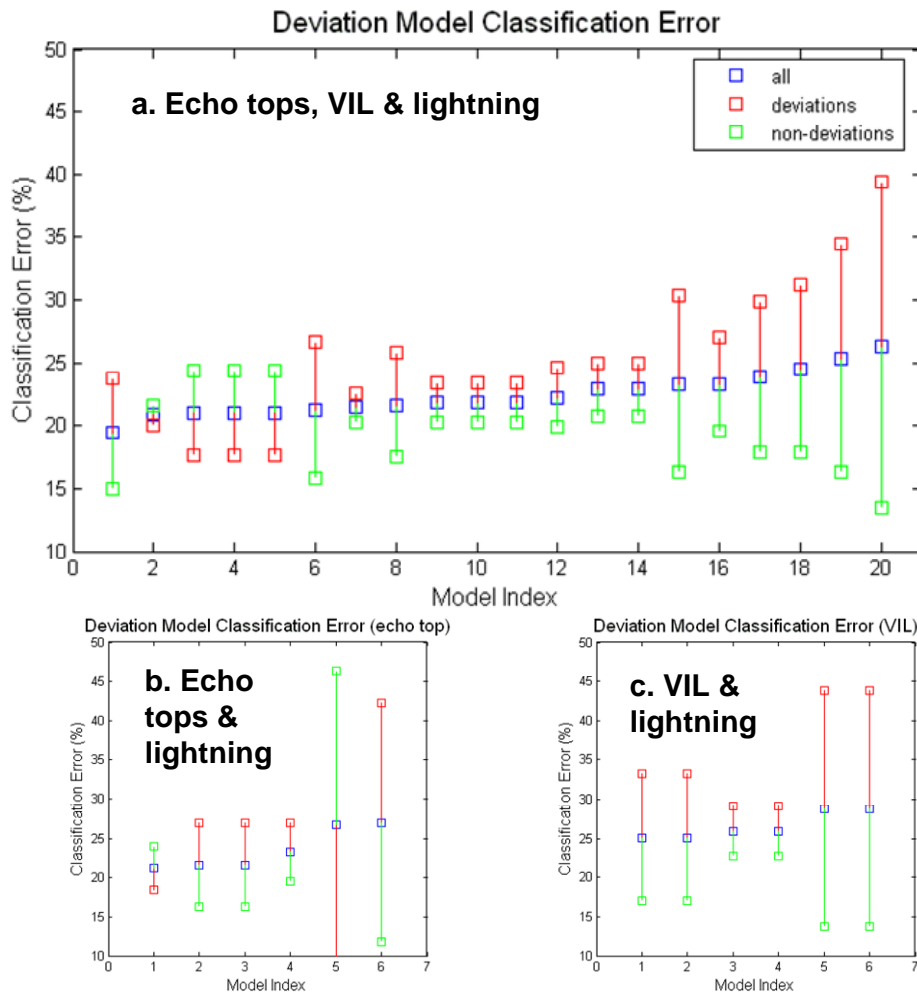


Figure 5. Summary of deviation prediction model errors. Figure (a) shows results for models with VIL, echo top height and lightning inputs, (b) shows results for echo top and lightning inputs, (c) for VIL and lightning inputs.

Figures 6 - 8 provide a more detailed look at the prediction model inputs and results for one of the models (model index 9, from Figure 5a). In this model, the five input predictors tested in the model were (1) flight altitude – 90th percentile echo top in the 16km neighborhood (deltaZ), (2) percentage of pixels in the 60km neighborhood whose VIL is level 3 or greater (L3PCT), (3) percentage of pixels in the 60 km neighborhood with echo tops >= 40kft, (4) 90th percentile VIL level in the 16 km neighborhood and (5) lightning counts in the 60km neighborhood. The best predictors of deviation were deltaZ and L3PCT.

Figure 6 shows three 2D histograms: deviation counts, non-deviation counts and observed probability of deviation (percentage of flights in each histogram bin that deviated). The histograms inputs are the two best predictors of deviation according to the deviation model: L3PCT (x axis) and deltaZ (y axis).

Figure 7 shows the relationship between the weather inputs and the result (deviation or not). Figure 7a is a table that ranks the inputs in order

of their predictive power, and the cumulative output classification error as each input is added to the model. In this model, using deltaZ alone results in a prediction error of 24.49%; adding L3PCT reduces the prediction error to 21.22%. The addition of the third, fourth or fifth inputs resulted in a small increase in prediction error.

Figures 7b and 7c show four histogram plots. The upper plots show the distribution of the deltaZ and L3PCT measurements for all weather encounters, partitioned into deviations and non-deviations. The bottom histogram is the distribution of correct and incorrect predictions of deviation and non-deviation. Correct predictions are above the x axis, incorrect ones are below.

An input will be a good predictor of deviation if the deviation and non-deviation distributions are well separated as they are for deltaZ (see Figure 7b). Where the deviation and non-deviation distributions overlap, prediction errors will be higher. Figures 7b and 7c illustrate this result: note the higher classification error counts for deltaZ between -5 and 5 kft (Figure 7b), and for L3PCT between 20% and 30% (Figure 7c).

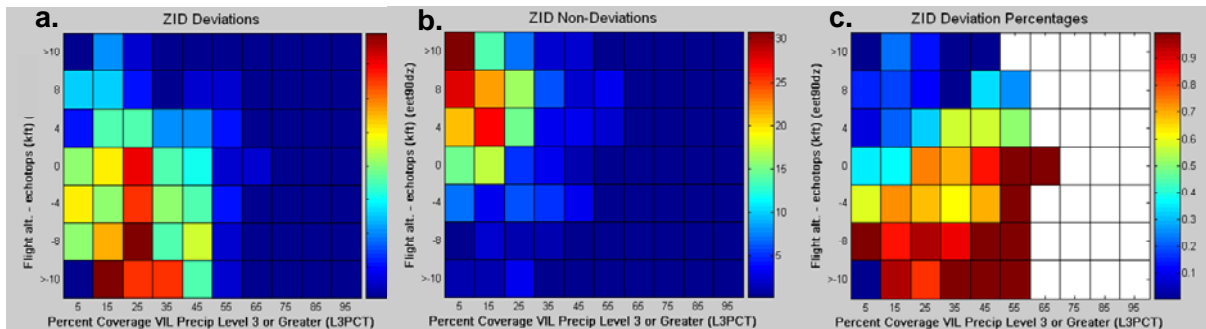
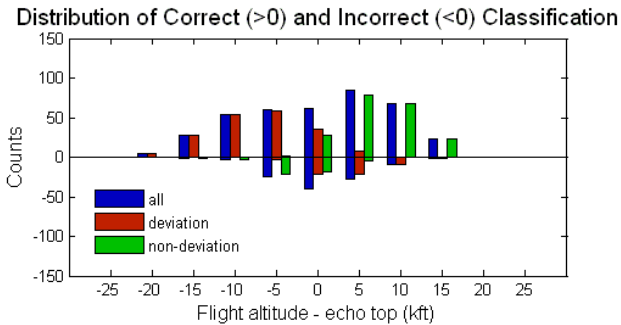
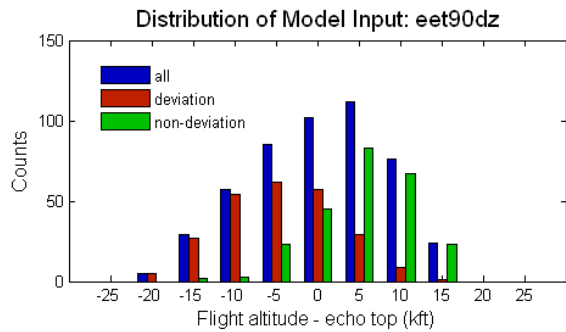


Figure 6. 2D histograms of deviation counts (a), non-deviation counts (b) and observed probability of deviation (percentage of flights in each histogram bin that deviated)(c). White bins in (c) indicate input data intervals that were not present in the encounter dataset (for example, no weather encounters were characterized by L3PCT between 70% and 100%).

a.

Weather input	Cumulative prediction error
deltaZ (flight alt. – 90th pct. echo top)	24.49%
% VIL pixels >= level 3	21.22%
% echo top pixels >= 40 kft	21.43%
90th pct. VIL	22.04%
Lightning counts	21.84%

b.



c.

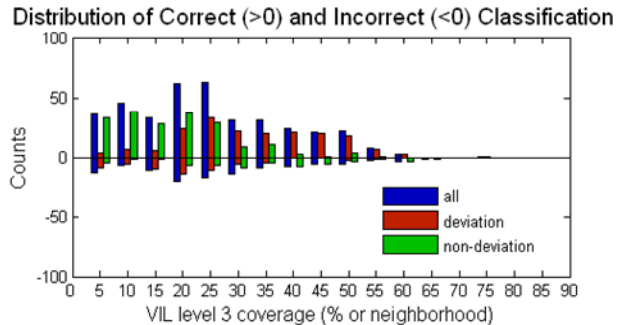
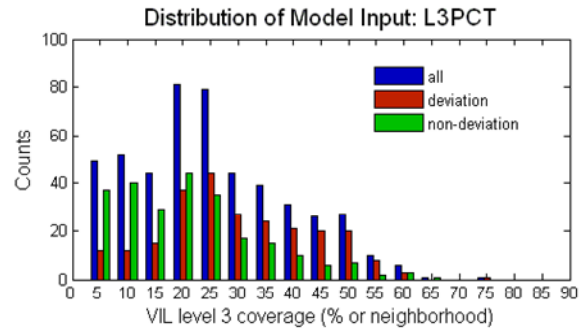


Figure 7. Relationship between weather inputs and deviation / non-deviation result. Table (a) ranks the weather inputs in order of explanatory power, with the cumulative deviation prediction error. Histogram (b) shows distribution of deltaZ for all weather encounters (blue), deviations (red) and non-deviations (green). Histogram (c) shows the same for VIL level 3 percent coverage.

Figure 8 is a scattergram of the two best predictor values (VIL level 3 percentage on the x axis, deltaZ on the y axis) for each weather encounter plotted on top of the decision regions determined by the deviation prediction model. Each point in the scattergram is colored to indicate if it was a deviation (gold) or not (red). The decision regions defined by the deviation prediction model are half-planes in the input space (deviation in gold and non-deviation in red). The deviation prediction for an input data point (i.e., a planned trajectory weather encounter) is determined by the decision region in which it falls. Planned trajectories whose deviation was incorrectly predicted by the model appear as 'speckle' (red boxes on the gold region or gold boxes on the red). Correct predictions appears as white-outlined boxes. Note that decision region boundaries may be suspect in regions where data is sparse – a model performs best where there is sufficient data!

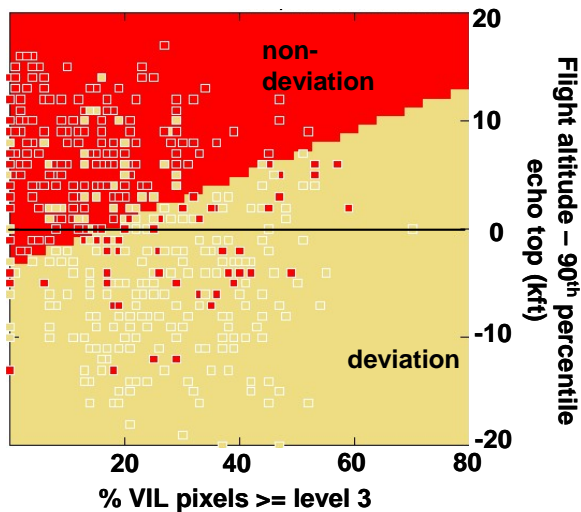


Figure 8. Deviation decision plot, as a function of weather input variables. X axis is percent of VIL pixels in the 60 km route region that are level 3 or greater. Y axis is deltaZ, (flight altitude – 90th percentile echo top height from the 16 km route region).

Finally, Figure 9 shows the histograms of lightning counts for all weather encounters, partitioned into deviations and non-deviations, for both ZID and ZOB. It is evident from the histograms that lightning counts in the 60 km neighborhood may provide some predictive skill, if data such as echo tops or VIL are not available.

4.3 Avoidance Distance Analysis

Avoidance distances were determined from a single characteristic cross-section specified by the analyst for each deviation. A second analyst reviewed the cross-sections, but the choice of a single cross-section to characterize the deviation strategy is somewhat subjective. In some instances, the analyst could not make a sensible choice of cross-section. Of the 248 verified deviations in ZID, cross-sections were selected from 220.

The data automatically extracted from the VIL and echo top fields along the cross-section define avoidance *distance curves*, which show VIL and echo top height as a function of position along the cross section. Using the point of intersection between the cross-section and the actual trajectory, the avoidance distance from different weather feature boundaries may be calculated automatically from the avoidance distance curve. Figure 10 illustrates an example.

Unfortunately, not all deviation strategies and avoidance distance determinations were as clear-cut as those illustrated in Figure 10. Figure 11 illustrates an example where neither the cause for deviation nor the deviation strategy is clear.

Of all 24 avoidance distances calculated, those for VIL level 2 and 3 features were the most consistent, implying that VIL level 2 or 3 contours may provide the best avoidance region boundary for deviating pilots. Approximately 75% of all deviating aircraft (168 of 218) flew within 20 km of the VIL level 2 boundary and within 25 km of the VIL level 3 boundary. This suggests a two step process to create a 'convective region avoidance field': (1) use flight altitude, echo tops and VIL to find regions that pilots will wish to avoid, (2) find the VIL level 2 or 3 contours that bound these regions.

It is important to note that one must use caution in interpreting the avoidance analysis data. It provides insights into pilot behavior that must be confirmed by analysis of a larger dataset. However, it deviation strategies may not be easily inferred from weather and trajectory data due to the complexity of convective weather and traffic patterns in busy airspace, the lack of concrete evidence about what information sources are used by the pilot and the fact that the deviation strategy may be imperfectly executed and therefore, the actual trajectory flown may not reflect the pilot's intent. More research is necessary to understand the specific relationships between weather, traffic and deviation strategies.

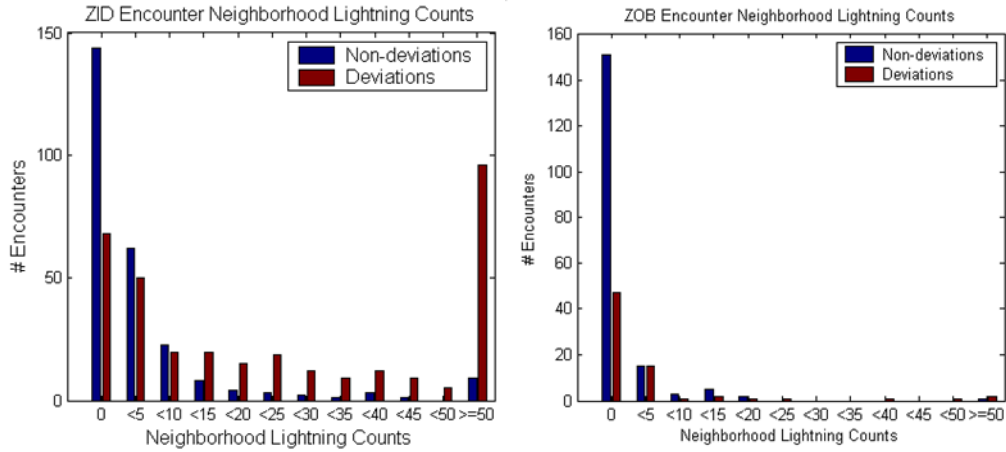


Figure 9. Histograms of lightning counts within the 60km encounter neighborhood box in the 6 minutes immediately prior to weather encounters in ZID and ZOB.

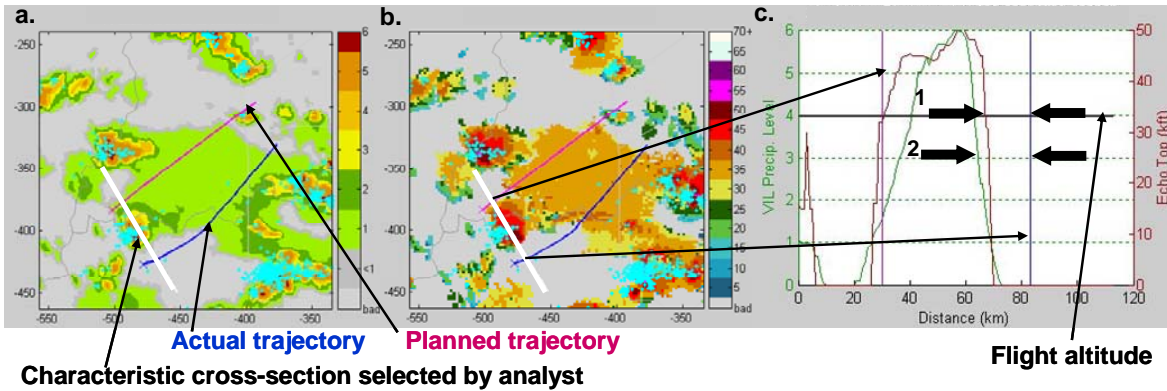


Figure 10. Avoidance distance analysis. Figure (a) shows the **planned** and **actual** trajectories from a deviation overlaid on the VIL field; Figure (b) shows the echo top field; Figure (c) shows the avoidance distance curves for VIL and echo tops along the characteristic cross-section. Arrows labeled (1) show the avoidance distance for echo top height equal to flight altitude, arrows (2) show avoidance of VIL level 3.

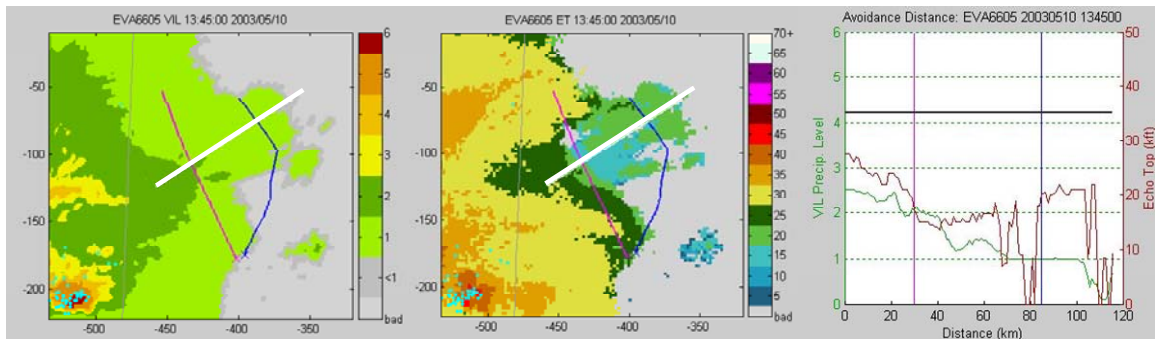


Figure 11. Illustration of an unclear deviation strategy. Pilot makes a large deviation in a region of benign weather, more than 100 km downwind from nearest convective cell.

4.4 Weather Penetration

Figure 12 summarizes the penetrations in the ZID super-sector for all case days; Figure 13 does the same for ZOB. The figures indicate that while most of the ‘penetrations’ are actually over-flights, a significant percentage of pilots are willing to penetrate regions of high echo tops and VIL that would be characterized as high

avoidance regions by the deviation prediction model. These results suggest that VIL and echo top height alone do not provide sufficient information about the vertical structure and dynamics (growth and decay) of convective cells – information that is often visible to pilots as they fly - to define completely regions of convective weather that pilots will wish to avoid.

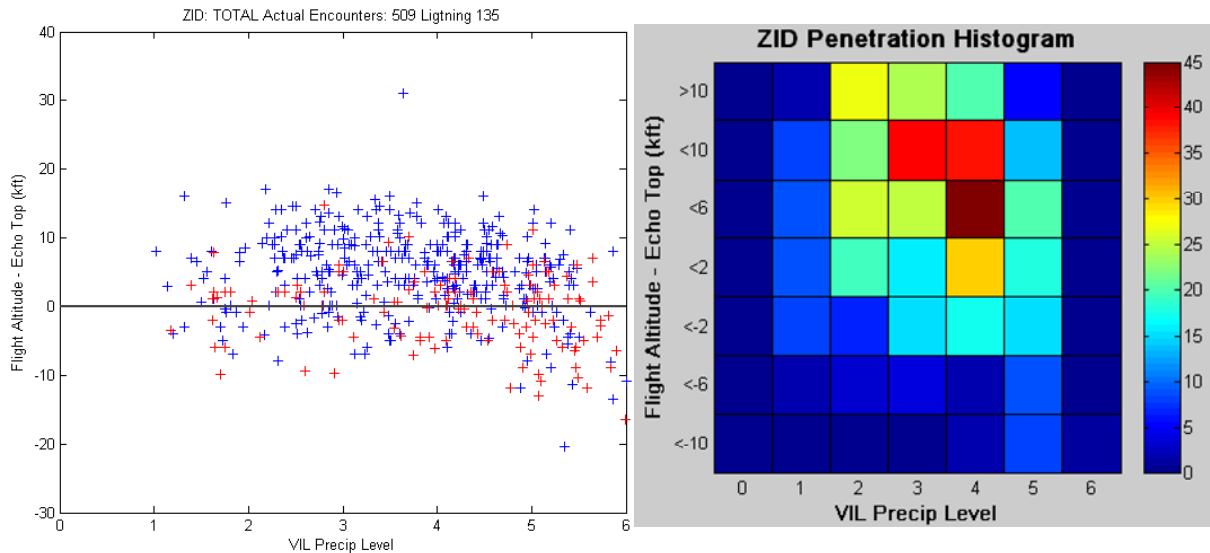


Figure 12. ZID penetrations. Scattergram at left shows plots deltaZ vs. VIL level for all actual trajectory weather encounters. Blue + indicate encounters where the neighborhood cloud to ground lightning count was <10; red + indicates counts ≥ 10 . Data points above the 0-line represent over-flights, where flight altitude > echo top height. Plot at right is the histogram of the weather encounter data.

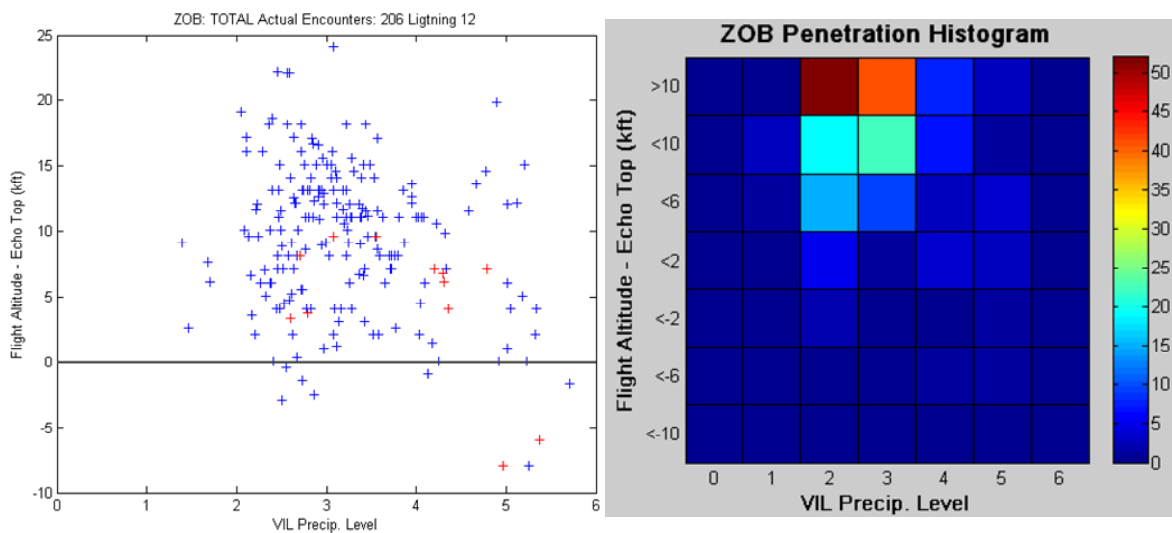


Figure 13. ZOB penetrations. Plots as in Figure 12.

5. SUMMARY, CONCLUSIONS AND ADDITIONAL WORK

This study presents the initial results in the development of a model to predict enroute flight deviations due to convective storms. The model was developed by applying statistical pattern recognition techniques to high resolution VIL and echo tops from CIWS and cloud-to-ground lightning strike counts from NLDN to characterize the weather, and flight plan and trajectory data from ETMS to determine planned and actual enroute flight trajectories and deviations. A model was also developed to describe avoidance distances from different weather features and weather penetration. Weather and flight data from over 800 different trajectories on five different days in two different air traffic control 'super-sectors' (ZID and ZOB) were analyzed.

A deviation prediction model could be developed only in the ZID super-sector, where the convective cells were generally strong and well-defined, a sufficient number of verified deviating and non-deviating flight trajectories were found and the difference between deviating and non-deviating flight trajectories was clear. The results of the modeling experiments were clear and consistent:

- 1) **Deviation prediction models with error rates for both deviations and non-deviations below 25% were possible, using several different sets of weather data measurements as inputs.**
- 2) **In all modeling experiments (except those with VIL only), *deltaZ* (the difference between flight altitude and echo top height) was the most powerful predictor of deviation.** The use of 90th percentile echo top measurements in the calculation of *deltaZ* resulted in lower errors than average values of echo top height.
- 3) **Measurements of VIL, without echo top heights, proved to be relatively poor predictors of deviation, when compared to models with echo tops only or both echo tops and VIL.** However, the combination of echo tops and VIL measurements in the input data set reduced the spread between errors in predicting deviations and non-

deviations from that achieved by using echo tops and lightning alone.

For all verified deviations, avoidance distances from 24 different weather features were calculated, where possible, based on input from an analyst. Avoidance distances for 220 deviations were analyzed. Seventy-five percent of deviating trajectories passed within 20 km of the level 2 boundary and within 25 km of the level 3 boundary. This suggests that a model for deviation strategy may use echo tops and VIL together to predict where planned trajectories will encounter regions of weather that the pilot will wish to avoid, and that the VIL level 2 or 3 contours surrounding those regions best defines the deviation distance.

Weather penetration statistics were also gathered for more than 700 weather encounters in both ZID and ZOB super-sectors. The data suggest that pilots are willing to fly over level 4 and even level 5 VIL if they can clear the echo tops by 4 - 6 kft, and that a significant percentage of pilots may penetrate regions of high echo top and VIL that would be determined to be likely avoidance regions by the deviation prediction model. This indicates that VIL and echo tops alone are probably not sufficient to define regions of convective weather that pilots will seek to avoid.

Finally, it must be noted that this is an **exploratory study**. The conclusions were limited by the small size of the input data set and the immaturity of the algorithms used to analyze trajectories and characterize weather encounters. We clearly need to examine many more convective weather cases in a number of different regions. For example, it is very important to determine if there are differences in pilot direction (e.g., ZOB, ZNY and possibly ZDC) versus ARTCCs where there is much greater distances between routs (e.g., ZID and ZME). ARTCCs that are principally transitional airspace (e.g., ZAU, ZTL, ZFW) may also have significantly different pilot behavior.

Several additional studies could provide key information that could improve deviation modeling:

- 1) **Improved definition and detection of deviation.** More work is needed to develop a better operational definition of deviation that considers factors not accounted for in this study, including sector route structure, prevalent ATC routing strategies and characteristics of convective weather.
- 2) **Addition of other relevant weather data.** Upper-level winds from RUC and storm

motion vectors from CIWS provide information necessary to determine if a planned or actual trajectory is downwind or upwind of a convective cell, or in front of or behind the path of a moving storm. Information about cell dynamics (growth and decay) and 3D reflectivity structure is also likely to be important. Operational evidence suggests that pilots may be more willing to penetrate regions with higher VIP levels on the trailing edge of a storm where cells are decaying, while avoiding lower VIP levels on the leading edge where cells are actively growing (DeLaura and Allan, 2003). It is also important to determine if there are differences in pilot behavior depending on the nature of the convective storm (squall line versus large scale airmass or other types of "disorganized" convection). PIREPs are also likely to affect pilot decisions in convective weather.

- 3) **Improved avoidance distance calculation algorithms.** The hazard avoidance distance calculation used in this study is compact and easily analyzed. However, it was labor intensive, provided only a small sampling of the available data and could not be applied to approximately 15% of all verified deviations, where complicated weather patterns resulted in deviation strategies that could not be characterized by a single avoidance distance.
- 4) **Inclusion of more factors in prediction of deviation strategies.** Deviation strategies most likely involve several factors not considered here: availability of clear airspace nearby, airspace constraints due to sector route geometry or traffic, etc.

6. REFERENCES

- DeLaura, Richard, and Allan Shawn, 2003, Route Selection Decision Support in Convective Weather: A Case Study of the Effects of Weather and Operational Assumptions on Departure Throughput, Budapest, Hungary, 5th Eurocontrol/FAA ATM R&D Seminar ATM-2003, <http://atm2003.eurocontrol.fr/>.
- FAA Aeronautical Information Manual, Feb. 17, 2005
- Lippmann, R.P., L. Kukolich L., and E Singer., 1993: *LNKnet Neural Network Machine Learning, and Statistical Software for Pattern Classification*, the Lincoln Laboratory Journal, Vol. 6, Num. 2.
- Mahoney, J., S. Seseske, J. E. Hart, M. P. Kay, and B. G. Brown, 2004: Defining observation fields for verification of the Collaborative Convective Forecast Product (CCFP): Part 2, Proceedings of the American Meteorological Society 11th Conference on Aviation, Range and Aerospace Meteorology, Hyannis, MA 2004.
- Rhoda, D.A., E.A. Kocab, M.L. Pawlak, 2002: "Aircraft encounters with convective weather in en route vs. terminal airspace above Memphis, Tennessee", 10th Conference on Aviation, Range and Aerospace Meteorology, American Meteorological Society, Portland, OR.
- Robinson, M. J., James Evans, Bradley A. Crowe, 2002: "En Route Weather Depiction Benefits of the NEXRAD Vertically Integrated Liquid Water Product Utilized by the Corridor Integrated Weather System", 10th Conference on Aviation, Range and Aerospace Meteorology, American Meteorological Society, Portland, OR.
- Robinson, M. J., Evans, B. Crowe, D. Klinge-Wilson, S. Allan, 2004: "Corridor Integrated Weather System Operational Benefits 2002-2003: Initial Estimates of Convective Weather Delay Reduction", MIT Lincoln Laboratory Project Report ATC-313.
- Smalley, David, Betty Bennett and Margita Pawlak, 2003, *New Products for the NEXRAD ORPG to Support FAA Critical Systems*, Long Beach, CA, 19th American Meteorological Society International Conference on Interactive Info Processing Systems for Meteorology, Oceanography and Hydrology.
- Troxel, S.D., and C.D. Engholm, 1990: "Vertical reflectivity profiles: Averaged storm structures and applications to fan beam radar weather detection in the U.S.", 16th Conference on Severe Local Storms, American Meteorological Society, Kananaskis Park, Alta, Canada.